Relationship between the tropical tropopause and tropical easterly jet streams over Indian monsoon region

Sanjay K. Mehta*, †, Vanmathi A, Saleem Ali, Aravindhavel A, and Ramesh Reddy

SRM Research Institute, SRM Institute of Science and Technology, Kattankulathur, 603203, India

*Corresponding author: Sanjay Mehta (ksanjaym@gmail.com)

†This work was partially carried out when the author was at National Atmospheric Research Laboratory (NARL), Gadanki, 517502, India

Key Points:

- Using radiosonde observations, we report the plausible relationship between tropical tropopause and tropical easterly jet (TEJ) streams.
- Cold point tropopause altitude and temperature are driven by adiabatic processes when TEJ core lies in the vicinity of tropical tropopause.
- It indicates that the TEJ plays an important role in the tropical tropopause variability which needs to be taken into account.

Abstract

This paper presents the first quantitative relationship between the cold point tropopause (CPT) and tropical easterly jet (TEJ) using radiosonde observations over Gadanki (13.45°N, 79.2°E) during the Indian summer monsoon season 2006–2014. CPT and TEJ peak altitudes (H_{CPT} and H_{TEJ}) show amalgams of two categories of variability on day to day scale. In category1 H_{TEJ} occurs close to H_{CPT} and they show in phase variation. While in category2 H_{TEJ} occurs far apart from H_{CPT} and they do not show any relationship. For category1 H_{CPT} and H_{TEJ} are strongly correlated (0.70) as well as H_{CPT} and T_{CPT} (CPT temperature) are moderately anticorrelated (-0.55) significant at 95% confidence level indicating the dominance of adiabatic processes. Whereas in category2 H_{CPT} and T_{CPT} are not significantly anticorrelated. Thus, when TEJ and CPT are close to each other it may serve as an indicator for the prevalence of synoptic-scale effect.

Plain Language Summary

During Indian summer monsoon (ISM) season tropical easterly jet (TEJ) streams develop in the upper troposphere. Several times TEJ core reaches the altitude very close to the cold point tropopause (CPT) and sometimes even penetrates the lower stratosphere. When CPT and TEJ are close to each other they vary in phase for several days continuously and are strongly correlated. It is well known that adiabatic processes dominate during the ISM season, which controls the day to day variability of the CPT altitude and temperature. In this study, we report that when TEJ is closer to CPT, adiabatic processes prevail. Thus, it indicates the relevance of the TEJ in the variability of the tropical tropopause which needs to be taken into account.

1 Introduction

Indian summer monsoon (ISM) is one of the dominant climatological features of the global circulation and it originates from the differential heating of the land and sea during summer season (Koteswaram, 1960). ISM brings several changes in the meteorological and dynamical features from the surface to the upper troposphere (UT). A noticeable feature in the UT is the development of the tropical easterly jet (TEJ) streams with speeds often exceeding 30 m/s. TEJ spans around the equator to 20^{o}N latitude and 50–90^{o}E latitude (Krishnamurti & Bhalme, 1976; Roja Raman et al., 2009). TEJ is a thermal wind maintained by the meridional temperature gradient between land and ocean (Hastenrath, 1995; Koteswaram, 1958). Other dominant features of the ISM are the shift of the intertropical convergence zone poleward, development of the low-level jet streams (Joseph & Sijikumar, 2004), increase in cloudiness and rainfall (Sikka & Gadgil, 1980) which leads to the enhancement in tropospheric humidity (Fasullo & Webster, 2003), and the increase in the frequency of deep convection which generally couples with the transport of the pollutants from the surface to the UT and lower stratosphere (LS; UTLS) (Garny & Randel, 2016). ISM can affect the UTLS thermal structure either directly due to diabatic heating associated with the convection or indirectly due to convectively generated phenomena such as propagation of atmospheric waves (Krishna Murthy et al., 2002; Tsuda et al., 1994), the occurrence of the cirrus clouds (Tseng & Fu, 2017) and transport of surface pollutants (Pan et al., 2016).

The tropical tropopause here is defined as the level of the coldest point in the UTLS called the cold point tropopause (CPT). CPT plays an important role in entry of the water vapor into the LS and hence regulates the climate variability (Gettelman et al., 2009; Holton et al., 1995). CPT shows connections with various tropospheric and stratospheric phenomena on different time scales. It has been linked with Madden Julian Oscillation (Zeng et al., 2012) and Brewer-Dobson

circulations (Birner, 2010) on a seasonal and annual scale, respectively. On the interannual scale, CPT shows connections with El Nino Southern Oscillation (Zhou et al., 2001) and quasi-biennial oscillations (Baldwin et al., 2001; Reid & Gage, 1985). On longer-term scale, an increase in the tropopause height was associated predominantly due to the increase in the well-mixed greenhouse gases (Santer et al., 2003).

Over the Indian monsoon region, 60% of the day to day variability of CPT (i.e. out of phase variation of the CPT height ($\boldsymbol{H_{CPT}}$) and temperature ($\boldsymbol{T_{CPT}}$)) is driven by adiabatic process (Mehta et al., 2010; Jain et al., 2011; Mehta et al., 2011) indicating a strong connection with ISM. The adiabatic process is due to hydrostatic adjustment to convective heating or cooling (Holloway & Neelin, 2007; Kim et al., 2018). While the in-phase variation of $\boldsymbol{H_{CPT}}$ and $\boldsymbol{T_{CPT}}$ is governed by the diabatic processes such as radiative heating/cooling from cirrus clouds (Hartmann et al., 2001; Boehm & Verlinde, 2000), turbulent mixing of the overshooting air with the environment (Sherwood et al., 2003, a large-scale westward propagating Rossby wave and eastward propagating Kelvin wave response (Highwood and Hoskins, 1998; Randel et al., 2003) or a combination of these. Recently, a link between the onset of ISM and tropical tropopause are observed (RavindraBabu et al., 2019). Kulkarni and Verma (1993) observed that the tropopause is at a higher altitude during active monsoon when compared to weak monsoon years (Varikoden & Preethi, 2013). TEJ core has been found in between the peaks of the frequency distribution of the tropopause altitudes obtained over a few stations in the ISM region (Ramanadham et al., 1969). Jain et al. (2011) observed that the occurrence of the extreme CPT was due to the westward propagating wave associated with TEJ. Fujiwara et al. (2003) observed a persistent temperature

inversion layer in the UT which they attributed to TEJ. Ratnam et al. (2011) noticed that sometimes TEJ penetrates to the LS which may lead to the transport of ozone into the UT.

Thus, TEJ has been associated with various studies such as occurrence of cirrus clouds (Das et al., 2011), gravity wave generation (Ramkumar et al., 2010; Sasi et al., 2000) and horizontal transport of the constituents (Orbe et al., 2015; Ploeger et al., 2017) which in turn may modify the CPT. However, to the best of our knowledge, no systematic study has been reported on the relationship between TEJ and CPT. Hence, here we make an attempt to understand the relationship between the day to day variability of the CPT and TEJ. The main objectives of the present study are to (i) investigate the plausible connection between $\boldsymbol{H_{CPT}}$ and $\boldsymbol{H_{TEJ}}$, and, (ii) delineate the effect of the TEJ on the relationship between $\boldsymbol{H_{CPT}}$ and $\boldsymbol{T_{CPT}}$.

2 Database

High-resolution radiosonde (Väisälä RS-80, Väisälä RS-92, and Meisei RS-06G) temperature and zonal wind profiles observed at around 1730 IST (IST = UT + 0530 h) over Gadanki (13.5°N, 79.2°E) during June-July-August (JJA) 2006-2014 are used in this study (www.narl.gov.in). These profiles are originally observed at height resolution ~ 25-30 m (sampled at 5 s intervals) which are uniformly gridded to 100 m. The uncertainties in temperature and wind speed given by the manufacturer are 0.2/0.3 K (below/above 100 hPa) and 0.15 m/s in Väisälä radiosonde (Vömel et ., 2007) and ±0.5 K and ±0.2 m/s in Meisei radiosonde, respectively (Kizu et al., 2018). We have only considered those soundings which have reached at least 50 hPa (Mehta et al., 2011) in order to obtain the altitude of CPT and TEJ. Globally merged infrared brightness temperature (IRBT) data obtained from national weather service Climate Prediction Centre, NOAA also used in the present study to examine the role of the convection of the relationship between TEJ and CPT. For our purpose, we have averaged the IRBT data into 0.5˚× 0.5˚ (latitude

– longitude) centered to Gadanki and within half-hour of 1730 IST. More details about IRBT data can be found in Mehta et al., (2017).

3 Results and Discussion

3.1 Typical observations- relationship between H_{CPT} and H_{TEJ}

After examining several hundred profiles it is found that H_{CPT} and H_{TEJ} occur very close to each other frequently and sometimes match. We have observed that both the temperature and zonal wind show similar structures just below and above the CPT in many of the profiles. Typical examples of comparison between H_{CPT} and H_{TEJ} are shown in Figures 1a – 1f for three different types of temperature profiles indicating the sharp, broad, and multiple tropopause cases, respectively. It is interesting to observe that the zonal wind profiles also show sharp, broad and multiple TEJ peaks similar to the temperature profiles. Figures 1a-b show the temperature and zonal wind profiles for the sharp case in which H_{CPT} and H_{TEJ} occur at the same altitude ~ 17.3 km observed on 02 July 2006. The T_{CPT} is found to be 194.5 K and TEJ core speed is -49.4 m/s.

Similarly, the temperature and zonal wind profiles are shown in Figures 1c–d depict the broad case in which the observed H_{CPT} and H_{TEJ} also occur at the same altitude ~ 17.2 km on 10 August 2008. The temperature remains almost constant (~ 190 K) between 16.5 –17.5 km characterizing a broad tropopause and the zonal wind is found to vary a little (~ – 37.8 to – 38.7 m/s) between altitude 16.8–17.7 km characterizing a broad TEJ. The typical case presented here shows that the broader tropopause is colder (by ~ 5 K) when compared to the sharp tropopause in contrast to the generally known fact that the tropopause is warmer and lower when compared to the sharper tropopause (Seidel et al. 2001; Schmidt et al. 2004; Kim and Son, 2012) which needs a detailed investigation; however, it is out of the scope of the present study.

An example of the double tropopauses and double peaks in the zonal wind is observed on 09 July 2010 as shown in Figures 1e – 1f. The temperature profile shows H_{CPT} at ~ 17.9 km and the Lower Tropopause (Mehta et al., 2011) at ~ 16.5 km. The zonal wind profile shows H_{TEJ} at ~ 17.6 km with a lower peak at altitude ~16.4 km similar to the temperature profile. These typical examples indicate that the zonal wind and temperature profiles around the tropopause behaves in a similar fashion which further indicates the possibility of a direct relationship between H_{CPT} and H_{TEJ} (Supplementary Fig. S1) .

Observed similar structures in the temperature and zonal wind around the tropopause region (Figure 1) are expected due to thermal wind balance. The thermal wind equation, which describes the relationship between the vertical gradient of zonal wind speed and the meridional gradient of temperature under hydrostatic equilibrium, is

$$\frac{\partial u}{\partial z} = -\frac{g}{fT}\frac{\partial T}{\partial y} \qquad (1)$$

Where u is the zonal wind, g is the acceleration due to gravity, f is Coriolis parameter and y is the northward distance (Andrews, 2010). It is observed that tropopause temperature gradient is greater (i.e. sharp tropopause) in the presence of relatively stronger zonal wind shear (Figures 1a-b) when compared to the cases when broad and multiple tropopauses are observed (Figures 1c-f). Also, the tropopause with broad and multiple structures are colder than the sharp tropopause. It is important to mention here that the warm (cold) air advection is associated with the wind which turns clockwise (counterclockwise) with height (Holton, 2004). The relatively warmer (colder) tropopause in the case of the sharper (broader and multiple) tropopause could be related to warm (cold) air advection due to the TEJ streams. The thermal wind balance due to TEJ streams is described in Supplementary Figure S2.

3.2 Temporal variation of H_{CPT} and H_{TEJ} and an approach to quantify its relationship

The temporal variability of H_{CPT} and H_{TEJ} on day to day scale during JJA 2006 is shown in Fig. 2a and for JJA 2007-2014 in the Supplementary Figures S3a-S10a, respectively. In general, H_{CPT} (H_{TEJ}) has a large day to day variability (Mehta et al., 2010; Ratnam et al., 2011) and varies in the range of 15.2–19 km (13–19 km) within the monsoon season itself. Though CPT is generally lower during JJA , it can occur as high as 19 km on a few occasions (Mehta et al., 2011). We have calculated H_{CPT} tendency (day-to-day difference) as shown in Supplementary Fig. S11a and observed that H_{CPT} remains unchanged for ~ 2% times while it increases (decreases) for ~ 52% (46%) times. Similarly H_{TEJ} remains unchanged for ~6% times while it decreases (increases) for ~ 48% (46%) times. H_{CPT} (H_{TEJ}) changes (absolute value) within 1 km, 1-2 km, 2-3 km, 3-4 km and >4 km ~ 38% (70%), 26% (19%), 17% (4%), 10% (1%) and 4% (0%) times, respectively (Figs S11a-b) indicating that H_{CPT} has larger day to day variability when compared to H_{TEJ}. It also means that H_{TEJ} is governed by synoptic-scale process while H_{CPT} is the balance between radiative and convective processes. Generally, H_{TEJ} fluctuates abruptly especially during early June when synoptic-scale forcing is weak (Figs 2a & S3a-S10a). We observed that H_{TEJ} often occurs closer to H_{CPT}, however, they coincide only ~6% times. The absolute difference between H_{CPT} and H_{TEJ} is found to be within 1 km, 1-2 km, 2-3 km and 3-4 km for about 63%, 20%, 9% and 2% times, respectively (Supplementary Fig S11c).

From Figures 2a and S3a-S10a, it is clear that the H_{CPT} and H_{TEJ}variability can be mainly classified into following two categories. In one category they either coincide or occur close to each other and vary in a similar phase. In the second category, they occur far apart and appear to vary out of phase. To quantify the relationship between H_{CPT} and H_{TEJ}, we have obtained their absolute difference ($\overline{\Delta H}_{CPT-TEJ}$) and the climatological mean $\overline{\Delta H}_{Clim}$ over JJA 2006-2014 as shown in Figure 2b (for JJA 2006) and Supplementary Figures S3b-S10b (for JJA 2007-2014). The $\overline{\Delta H}_{Clim}$

is found to be 0.85 km. It is observed that the days during which H_{CPT} and H_{TEJ} are close to each other (far apart), $\overline{\Delta H}_{CPT-TEJ}$ occurs below (above) the $\overline{\Delta H}_{Clim}$. Generally, H_{CPT} and H_{TEJ} "close to each other" and "far apart" occur in a group. After examining all these cases, the following criterion is evolved for defining the relationship between H_{CPT} and H_{TEJ}. The days during which $\overline{\Delta H}_{CPT-TEJ}$ is lower (greater) than the $\overline{\Delta H}_{Clim}$ for three consecutive days or more are classified as category1 (category2). As CPT has a structure and may coincide TEJ for isolated (one or two) days randomly hence three days or more are considered to represent a synoptic-scale feature. For JJA 2006 five episodes of category1 and three episodes of category2 are observed (Figs 2a-b).

However, as we know that tropopause structure can be significantly modified due to convection (Sherwood et al., 2003; Muhsin et al., 2018) and associated planetary wave propagation (Boehm and Verlinde, 2000; Munchak and Pan, 2014), their possible roles in association with relationship between CPT and TEJ are also analyzed. The presence of the convective activities is investigated using IRBT data as shown in Fig 2c and Figs. S3c-S10c. From Fig 2, it is observed that H_{CPT} are affected due to deep convection activities. However, both category1 and category2 occur during the clear sky days as well as convective days indicating that the relationship between H_{CPT} and H_{TEJ} is not always linked to local convection and appears to be a response of large-scale synoptic condition (Supplementary Fig. S12). To examine the role of planetary wave, the continuous timeseries of the temperature anomalies averaged over 16-17 km observed from 26 June -22 August 2006 is subjected to Morlet wavelet analysis (Figure 2d). It is seen that the waves with periods 8–12 days are significant (above the cone of influence) during 20 July to 09 August 2006 during which H_{CPT} coincides with H_{TEJ}. However, they also coincide other timings irrespective of the wave occurrence. The wavelet analysis for JJA 2008-2014 is shown in

Supplementary Figs S4d-S10d except JJA 2007 which has a large data gap. The one-day data gaps are filled by linear interpolation to have continuous times for the wavelet analysis.

3.3 Statistical analysis of the relationship between TEJ and CPT: Plausible link with adiabatic and diabetic processes

In total 707 days observations of H_{CPT} and H_{TEJ} are available out of 828 days during JJA 2006–2014. After filling one day data gap, in total 731 days data are available for the analysis. Out of which 471 (65%) days and 260 (35%) days are observed for the cases when H_{CPT} and H_{TEJ} are "close to each other" and "far apart" respectively. Among these "close to each other" cases, 352 (76%) are found under category1 and the remaining 115 (24%) cases are found to be isolated. Similarly, among all these "far apart" cases 114 (44%) are observed under category 2 and rest 146 (56%) cases are found to be isolated. Figures 3a–c show the probability distribution of the difference between H_{CPT} and H_{TEJ} (hereafter $\Delta H_{CPT-TEJ}$) for overall monsoon season, category1 and category2, respectively. $\Delta H_{CPT-TEJ}$ ranges from –2.9 to 4.0 km (overall monsoon), between –0.9 to 0.9 km (category1) and between –2.9 to -1.0 km and 1 to 4 km (category2). The overall probability distribution of $H_{CPT-TEJ}$ indicates that 60% and 34% times TEJ occurs above and below the CPT, respectively while remaining 6% times coincides with CPT. For the category1, TEJ occurs 46 % (48%) times and below (above) the CPT whereas for category 2, 89% (11%) times TEJ occurs below (above) the CPT. The peak or mode (mean and standard deviation) of the distribution is found to be ~0.0 km (0.54±1.1 km), -0.2 km (0.06±0.43 km) and ~2.5 km (1.67±1.4 km) for overall monsoon season, category1 and category2, respectively.

Figures 3d–f show the scatter plots of H_{CPT} and H_{TEJ} indicating the random relationship in the overall data while they are strongly correlated (r = 0.70) significant at 95% confidence level under the category1 and no correlation under the category2. Note that when considering all the

H_{CPT} and H_{TEJ} "close to each other" and "far apart" cases, results remain the same (Figs 3e-f). A good correlation between H_{CPT} and H_{TEJ} under the category1 indicates TEJ is linked to the variation of the CPT. That is if TEJ lies in the tropopause vicinity influences the H_{CPT} variabilities. In category2, TEJ does not affect the CPT variability.

Figures 3g–i show the scatter plots of T_{CPT} and H_{TEJ} for overall monsoon data, category1 and category2, respectively. In the overall monsoon data, T_{CPT} and H_{TEJ} are moderately anticorrelated (r = –0.32) significant at 95% confidence level (Figure 3g) unlike the correlation between H_{CPT} and H_{TEJ}. It indicates that T_{CPT} is more sensitive to tropospheric processes especially infrared warming and therefore tropospheric temperature profile (Thuburn & Craig, 2000). Whereas the weak correlation observed between H_{CPT} and H_{TEJ} in overall monsoon data (Figure 3d) indicates that H_{CPT} is more sensitive to the ozone heating and dynamical warming (Thuburn & Craig, 2000) associated with stratospheric meridional circulation (Yulaeva et al., 1994). T_{CPT} and H_{TEJ} are moderately anticorrelated (r = –0.55) significant at 95% confidence level and weakly anticorrelated (r = -0.16) but not significant under the category1 and category2, respectively (Figures 3h-i). Thus, day to day variability of H_{CPT} , T_{CPT} and H_{TEJ} are linked under the category1.

It is interesting to observe that H_{CPT} and T_{CPT} are moderately anticorrelated in the overall monsoon season (r = –0.36) as well as under the category1 (r = –0.55) significant at 95% confidence level while weakly anticorrelated (r = –0.20) but not significant under the category2 as shown in Figures 3j-l. Thus, it appears that the adiabatic process is prominent when TEJ is nearby the CPT. However, H_{CPT} and T_{CPT} may not always be driven by adiabatic processes alone and can be affected by diabatic processes such as dynamical heating, ozone heating and occurrence of cirrus clouds (Mehta et al., 2010; Reid & Gage, 1996; Thuburn & Craig, 2000) which may be

241 dominant in controlling CPT variability when TEJ occurs far away from CPT. The above findings
242 are also consistent with analysis of each monsoon season from 2006 to 2014 except for 2011 and
243 2014 listed in the supplementary tables ST1 and ST2.

244 **3.4 Mean temperature and zonal wind profiles for overall, under category 1 and**
245 **category 2**

246 Figure 4 presents the mean and standard deviation of the temperature and zonal wind
247 profiles during the overall monsoon season, under the category1 and category2. On an average
248 T_{CPT} (~193 K) almost remains the same and TEJ peak speed (~ 35-39 m/s) shows a little variation
249 among overall monsoon season and the two categories. Whereas, H_{CPT} (H_{TEJ}) is at 16.6 km (16.2
250 km), 16.5 km (16.3 km) and 16.9 km (15.6 km) in overall monsoon season, category1 and
251 category2, respectively. Note that the mean H_{CPT} (T_{CPT}) obtained by averaging the daily values
252 are found to be 16.8±0.6 km (191.4±2.1 K) for overall data, 16.6±0.5 km (191.4±2.0 K) for
253 category1 and 17.1±0.6 km (191.4±2.0 K) for category 2 which are relatively higher by 0.1 – 0.2
254 km (colder by ~ 2.0 K) when compared to those obtained from the corresponding mean profiles.
255 TEJ peak speed and H_{TEJ} obtained from averaging daily data are found to be 40.7±6.9 m/s and
256 16.3±0.9 km for overall data, -42.1±6.7 m/s and 16.5±0.6 km for category1 and -40.0±6.7 m/s and
257 15.5±1.3 km for category2 which are also relatively faster by ~ 3 – 5 m/s and higher by ~ 0.1 – 0.2
258 km respectively when compared to those obtained from the mean profile. It indicates that results
259 for overall, category1 and category2 obtained from the mean profiles and individual profiles
260 remain consistent. On average TEJ occurs 0.2 km (1.3 km) below the CPT under the category1
261 (category2). Both temperature and zonal wind profiles have sharper peaks under the category1
262 whereas under the category2 they are relatively broader. Also, TEJ becomes relatively stronger
263 when it is closer to the CPT which can enhance the troposphere-stratosphere exchange processes

due to horizontal advection (Holton et al., 1995; Park et al., 2007; Das et al., 2011). The probability distribution of T_{CPT} indicates that $T_{CPT} < 191$K occurs more frequently under the category1 when compared to category2 (Figure not shown). Therefore, entry of water vapor from the troposphere to the stratosphere with the mixing ratio less than 3 ppmv is likely to occur more frequently in category1.

4 Summary and Conclusions

TEJ shows a large day to day variability which is expected because of variation in the meridional temperature gradient due to ISM variability. About 65% times of the total observations H_{TEJ} and H_{CPT} occurs "close to each other" and 35% times occur "far apart". Out of these "close to each other" cases, 76% times they occur continuously for three days or more (category1) during which adiabatic processes dominate. Finding from this study has far-reaching implications in understanding the variability and trend of surface energy balance and stratospheric chemistry due to enhanced cross-tropopause transport of the surface pollutants via Asian summer monsoon anticyclone (Pan et al., 2016; Mehta et al., 2020). The plausible relationship between H_{CPT} and H_{TEJ} investigated over a tropical station Gadanki using high-resolution daily radiosonde observations (JJA 2006-2014) are summarized below:

1. The effect of the TEJ is observed in the CPT when they occur close to each other. H_{TEJ} and H_{CPT} show in phase variation and are significantly correlated under this category. Whereas TEJ does not affect CPT when they are far apart.

2. When CPT and TEJ are close to each other, H_{CPT} and T_{CPT} are significantly anticorrelated indicating the prevalence of the adiabatic processes, whereas when they are far apart, no relationship found between them indicating the dominance of the diabatic processes.

3. Thus, when TEJ and CPT are close to each other it can serve as an indicator for the dominance of adiabatic processes.

Acknowledgments

We thank Director, NARL Gadanki, for providing the radiosonde data and NARL technical staffs for smoothly conducting the radiosonde observations. The radiosonde data used in this study is available from dropdown "View & Download Data" listed on the "Data/Experiment" tab of the NARL website (www.narl.gov.in). Information on how to download the radiosonde data is also provided in the supplementary material. IRBT data can be obtained from NASA Goddard Earth Sciences Data and Information Services Center (GES DISC). This work is fully supported by Department of Science and Technology- Science and Engineering Research Board (EMR/2015/000525).

References

Andrews, D. G. (2010). *An introduction to atmospheric physics*: Cambridge University Press.

Baldwin, M., Gray, L., Dunkerton, T., Hamilton, K., Haynes, P., Randel, W., et al. (2001). Marquardt C. andSato, K., Takahashi, M.: The quasibiennial oscillation. *Rev. Geophys, 39*(2), 179-229.

Birner, T. (2010). Residual circulation and tropopause structure. *Journal of the Atmospheric Sciences, 67*(8), 2582-2600.

Boehm, M. T., and Verlinde, J.: Stratospheric influence on upper tropospheric tropical cirrus. *Geophys. Res. Lett*., 27, 19, 3209-3212, 2000

Das, S. K., Chiang, C. W., & Nee, J. B. (2011). Influence of tropical easterly jet on upper tropical cirrus: An observational study from CALIPSO, Aura-MLS, and NCEP/NCAR data. *Journal of Geophysical Research: Atmospheres, 116*(D12).

Fasullo, J., & Webster, P. (2003). A hydrological definition of Indian monsoon onset and withdrawal. *Journal of Climate, 16*(19), 3200-3211.

Fujiwara, M., Xie, S. P., Shiotani, M., Hashizume, H., Hasebe, F., Vömel, H., et al. (2003). Upper-tropospheric inversion and easterly jet in the tropics. *Journal of Geophysical Research: Atmospheres, 108*(D24).

Garny, H., & Randel, W. J. (2016). Transport pathways from the Asian monsoon anticyclone to the stratosphere. *Atmospheric Chemistry and Physics, 16*(4), 2703-2718.

Gettelman, A., Birner, T., Eyring, V., Akiyoshi, H., Bekki, S., Brühl, C., et al. (2009). The tropical tropopause layer 1960–2100. *Atmospheric Chemistry and Physics, 9*(5), 1621-1637.

Gettelman, A. and de F. Forster, P. M.: A climatology of the Tropical Tropopause Layer. *J. Meteorol. Soc. Japan*, 80, 911-924, 2002

Hastenrath, S. (1995). Recent advances in tropical climate prediction. *Journal of Climate, 8*(6), 1519-1532.

Holton, J. (2004). An Introduction to Dynamic Meteorology (; Amsterdam. In: Elsevier.

Holton, J. R., Haynes, P. H., McIntyre, M. E., Douglass, A. R., Rood, R. B., & Pfister, L. (1995). Stratosphere-troposphere exchange. *Reviews of geophysics, 33*(4), 403-439.

Jain, A., Panwar, V., Johny, C., Mandal, T., Rao, V., Gautam, R., & Dhaka, S. (2011). Occurrence of extremely low cold point tropopause temperature during summer monsoon season: ARMEX campaign and CHAMP and COSMIC satellite observations. *Journal of Geophysical Research: Atmospheres, 116*(D3).

Joseph, P., & Sijikumar, S. (2004). Intraseasonal variability of the low-level jet stream of the Asian summer monsoon. *Journal of Climate, 17*(7), 1449-1458.

Kim, J., Randel, W. J., & Birner, T. (2018). Convectively driven tropopause-level cooling and its influences on stratospheric moisture. *Journal of Geophysical Research: Atmospheres, 123*(1), 590-606.

Kizu N, Sugidachi T, Kobayashi E, Hoshino S, Shimizu K, Maeda R, Fujiwara M (2018) Technical characteristics and GRUAN data processing for the Meisei RS-11G and iMS-100 radiosondes, GRUAN-TD-5, p 152. https ://www.gruan .org/docum entat ion/gruan /td/graun -td-5/

Koteswaram, P. (1958). The easterly jet stream in the tropics. *Tellus, 10*(1), 43-57.

Koteswaram, P. (1960). The Asian summer monsoon and the general circulation over the tropics. *Monsoons of the World*, 105-110.

Krishna Murthy, B., Satheesan, K., Parameswaran, K., Sasi, M., Ramkumar, G., Bhavanikumar, Y., et al. (2002). Equatorial waves in temperature in the altitude range 4 to 70 km. *Quarterly Journal of the Royal Meteorological Society, 128*(581), 819-837.

Krishnamurti, T. N., & Bhalme, H. (1976). Oscillations of a monsoon system. Part I. Observational aspects. *Journal of the Atmospheric Sciences, 33*(10), 1937-1954.

Kulkarni, J., & Verma, R. (1993). On the spatio-temporal variations of the tropopause height over india and indian summer monsoon activity. *Advances in atmospheric sciences, 10*(4), 481-488.

Meenu, S., Rajeev, K., Parameswaran, K., Nair, A.K.M., 2010. Regional distribution of deep clouds and cloud top altitudes over the Indian subcontinent and the surrounding oceans. *Journal of Geophysical Research: Atmospheres* 115 (D5).

Mehta, S. K., Ratnam, M. V., & Krishna Murthy, B. (2011). Multiple tropopauses in the tropics: A cold point approach. *Journal of Geophysical Research: Atmospheres, 116*(D20).

Mehta, S. K., Venkat Ratnam, M., & Krishna Murthy, B. (2010). Variability of the tropical tropopause over Indian monsoon region. *Journal of Geophysical Research: Atmospheres, 115*(D14).

Mehta, S. K., Fujiwara, M., Tegtmeier, S., Ratnam, M. V., Fadnavis, S., Santee, M., and Schlager, H. (2020). International Conference on the Asian Summer Monsoon Anticyclone: Gateway of Surface Pollutants to the stratosphere, *SPARC Newsletter No. 55,* August 2020, 21-25 pp., available at http://www.sparc-climate.org/publications/newsletter

Mehta, S. K., Venkat Ratnam, M., Sunilkumar, S.V., Narayana Rao, D., Krishna Murthy, B.V., Diurnal variability of the atmospheric boundary layer height over a tropical station in the Indian monsoon region, *Atmospheric Chemistry and Physics*, 2017, 17, 531-549

Muhsin, M., Sunilkumar, S. V., Venkat Ratnam, M., Parameswaran, K., Krishna Murthy, B., and Emmanuel, M.: Effect of convection on the thermal structure of the troposphere and lower stratosphere including the tropical tropopause layer in the South Asian monsoon region. *J.Atmospheric Sol.-Terr. Phys*., 169, 52-65, https://doi.org/10.1016/j.jastp.2018.10.016, 2018

Munchak, L. A., and Pan, L. L., Separation of the lapse rate and the cold point tropopauses in the tropics and the resulting impact on cloud top-tropopause relationships. *J. Geophys. Res.Atmos.*, 119, 7963-7978, doi:10.1002/2013JD021189, 2014

Orbe, C., Waugh, D. W., & Newman, P. A. (2015). Air-mass origin in the tropical lower stratosphere: The influence of Asian boundary layer air. *Geophysical Research Letters, 42*(10), 4240-4248.

Pan, L. L., Honomichl, S. B., Kinnison, D. E., Abalos, M., Randel, W. J., Bergman, J. W., & Bian, J. (2016). Transport of chemical tracers from the boundary layer to stratosphere associated with the dynamics of the Asian summer monsoon. *Journal of Geophysical Research: Atmospheres, 121*(23).

Ploeger, F., Konopka, P., Walker, K., & Riese, M. (2017). Quantifying pollution transport from the Asian monsoon anticyclone into the lower stratosphere. *Atmospheric Chemistry and Physics, 17*(11), 7055-7066.

Ramanadham, R., Subbaramayya, I., Rao, N. J., & Patnaik, J. (1969). The tropopause over India. *pure and applied geophysics, 75*(1), 355-364.

Ramkumar, T., Niranjan Kumar, K., & Mehta, S. K. (2010). Mesosphere-stratosphere-troposphere radar observations of characteristics of lower atmospheric high-frequency gravity waves passing through the tropical easterly jet. *Journal of Geophysical Research (Atmospheres), 115*(D14).

Ratnam, M. V., Raman, M. R., Mehta, S. K., Nath, D., Krishnamurthy, B., Rajeevan, M., et al. (2011). Sub-daily variations observed in Tropical Easterly Jet (TEJ) streams. *Journal of Atmospheric and Solar-Terrestrial Physics, 73*(7-8), 731-740.

RavindraBabu, S., Venkat Ratnam, M., Basha, G., & Krishnamurthy, B. (2019). Indian summer monsoon onset signatures on the tropical tropopause layer. *Atmospheric Science Letters*, e884.

Reid, G., & Gage, K. (1996). The tropical tropopause over the western Pacific: Wave driving, convection, and the annual cycle. *Journal of Geophysical Research: Atmospheres, 101*(D16), 21233-21241.

Reid, G. C., & Gage, K. S. (1985). Interannual variations in the height of the tropical tropopause. *Journal of Geophysical Research: Atmospheres, 90*(D3), 5629-5635.

Roja Raman, M., Jagannadha Rao, V., Venkat Ratnam, M., Rajeevan, M., Rao, S., Narayana Rao, D., & Prabhakara Rao, N. (2009). Characteristics of the Tropical Easterly Jet: Long-term trends and their features during active and break monsoon phases. *Journal of Geophysical Research: Atmospheres, 114*(D19).

Santer, B. D., Wehner, M. F., Wigley, T., Sausen, R., Meehl, G., Taylor, K., et al. (2003). Contributions of anthropogenic and natural forcing to recent tropopause height changes. *science, 301*(5632), 479-483.

Sasi, M., Ramkumar, G., Deepa, V., & Murthy, B. K. (2000). Inertia-gravity waves associated with the tropical easterly jet over the Indian subcontinent during the South West Monsoon Period. *Geophysical research letters, 27*(19), 3201-3204.

Sherwood, S. C., Horinouhi, T., and Zeleznik, H. A.: Convective Impact on Temperatures Observed near the Tropical Tropopause. *J. Atmos. Sci.,* 60, 1847-1855, 2003

Sikka, D., & Gadgil, S. (1980). On the maximum cloud zone and the ITCZ over Indian, longitudes during the southwest monsoon. *Monthly Weather Review, 108*(11), 1840-1853.

Thuburn, J., & Craig, G. C. (2000). Stratospheric influence on tropopause height: The radiative constraint. *Journal of the atmospheric sciences, 57*(1), 17-28.

Tseng, H. H., & Fu, Q. (2017). Temperature control of the variability of tropical tropopause layer cirrus clouds. *Journal of Geophysical Research: Atmospheres, 122*(20), 11,062-011,075.

Tsuda, T., Murayama, Y., Wiryosumarto, H., Harijono, S. W. B., & Kato, S. (1994). Radiosonde observations of equatorial atmosphere dynamics over Indonesia: 1. Equatorial waves and diurnal tides. *Journal of Geophysical Research: Atmospheres, 99*(D5), 10491-10505.

Varikoden, H., & Preethi, B. (2013). Wet and dry years of Indian summer monsoon and its relation with Indo-Pacific sea surface temperatures. *International journal of climatology, 33*(7), 1761-1771.

V¨omel, H., D. E. David, and K. Smith, Accuracy of tropospheric and stratospheric water vapor mea-surements by the cryogenic frost point hygrometer: Instrumental details and observations. *J. of Geophys. Res. Atmos.*,112(D8), D08,305, 10.1029/2006jd007224, 2007.

Wallace, J. M., & Hobbs, P. V. (2006). *Atmospheric science: an introductory survey* (Vol. 92). Elsevier.

Yulaeva, E., Holton, J. R., & Wallace, J. M. (1994). On the cause of the annual cycle in tropical lower-stratospheric temperatures. *Journal of the atmospheric sciences, 51*(2), 169-174.

Zeng, Z., Ho, S. P., Sokolovskiy, S., & Kuo, Y. H. (2012). Structural evolution of the Madden-Julian Oscillation from COSMIC radio occultation data. *Journal of Geophysical Research: Atmospheres, 117*(D22).

Zhou, X. L., Geller, M. A., & Zhang, M. H. (2001). Tropical cold point tropopause characteristics derived from ECMWF reanalyses and soundings. *Journal of climate, 14*(8), 1823-1838.

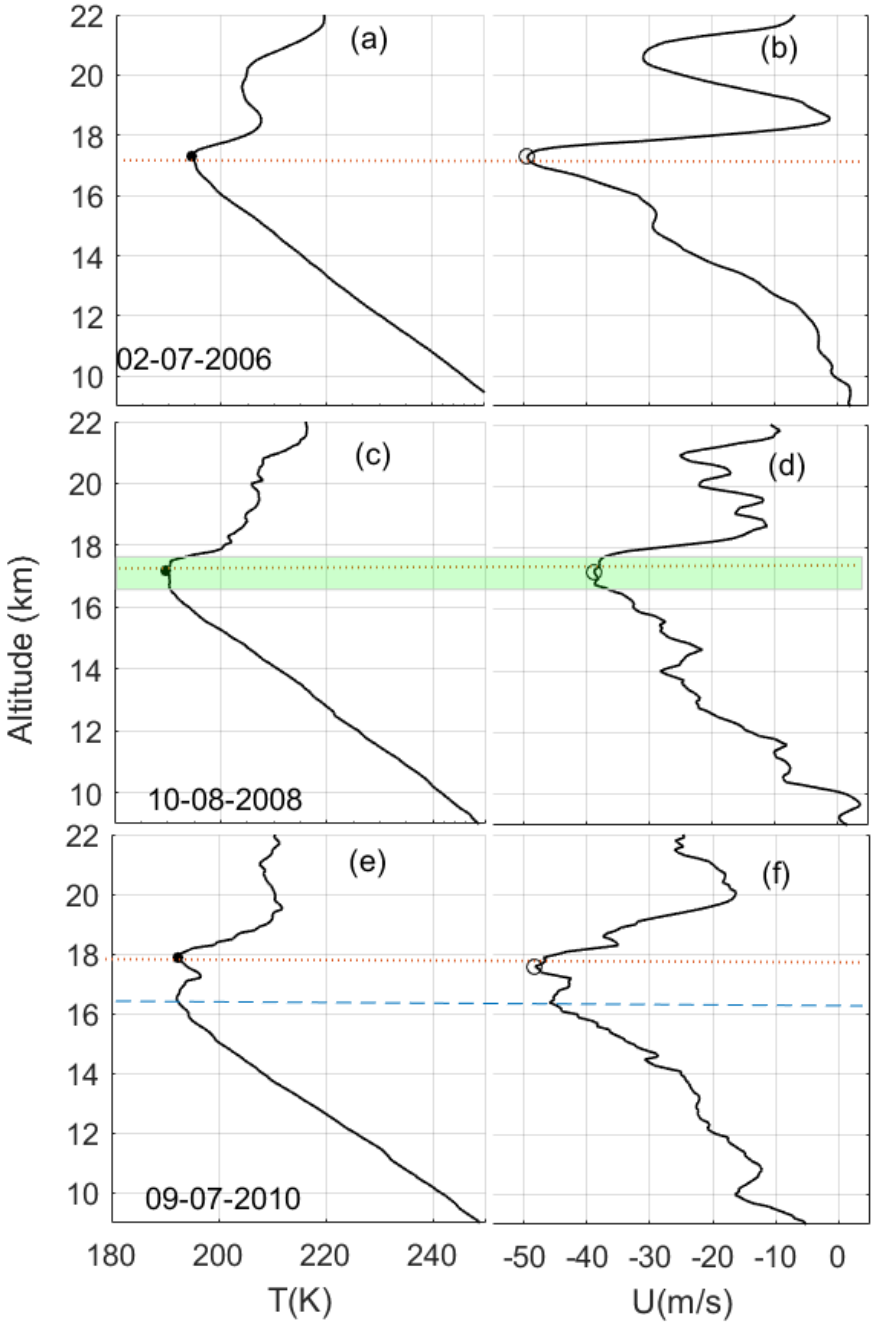

Figure 1. Typical temperature and zonal wind profiles showing (a-b) sharp tropopause and TEJ observed on 02 July 2006. (c – f) and (e – f) are the same (a-b) but observed on 12 June 2010 and 09 July 2010 showing broad and multiple tropopauses and TEJ cases, respectively. Solid dots and open circles denote the H_{CPT} and H_{TEJ},respectively.

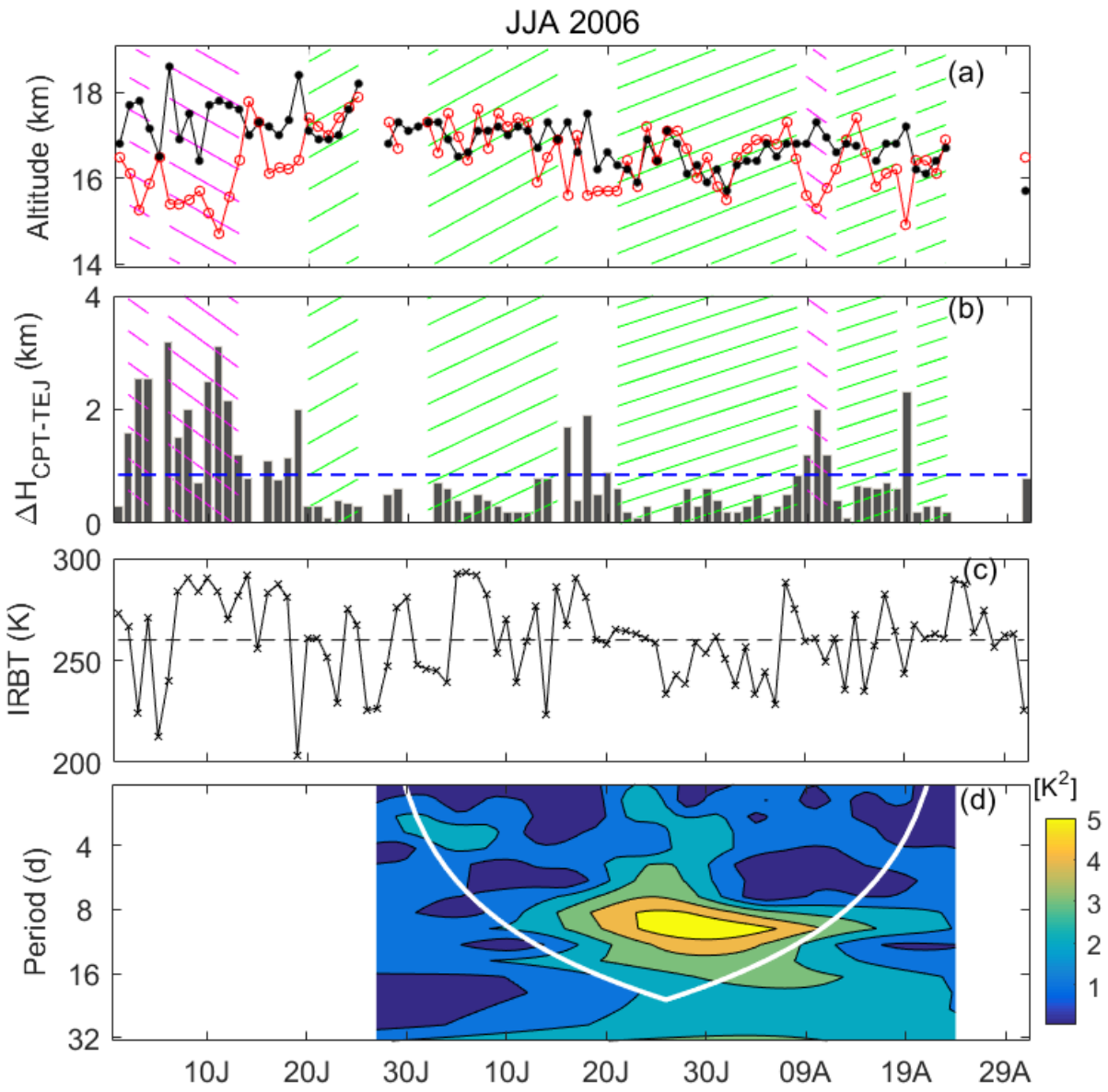

Figure 2. Time series of (a) H_{CPT} and H_{TEJ}, (b) $\overline{\Delta H}_{CPT-TEJ}$ (c) IRBT and (d) wavelet spectrum of temperature (in terms of power) at 16-17 km during JJA 2006. The up (green) and down(magenta) hatches indicate the catogory1 (category2) case. Horizontal dashed line in (b) represents $\overline{\Delta H}_{Clim}$ over the period 2006-2014 and white curve in (d) represents the cone of influence.

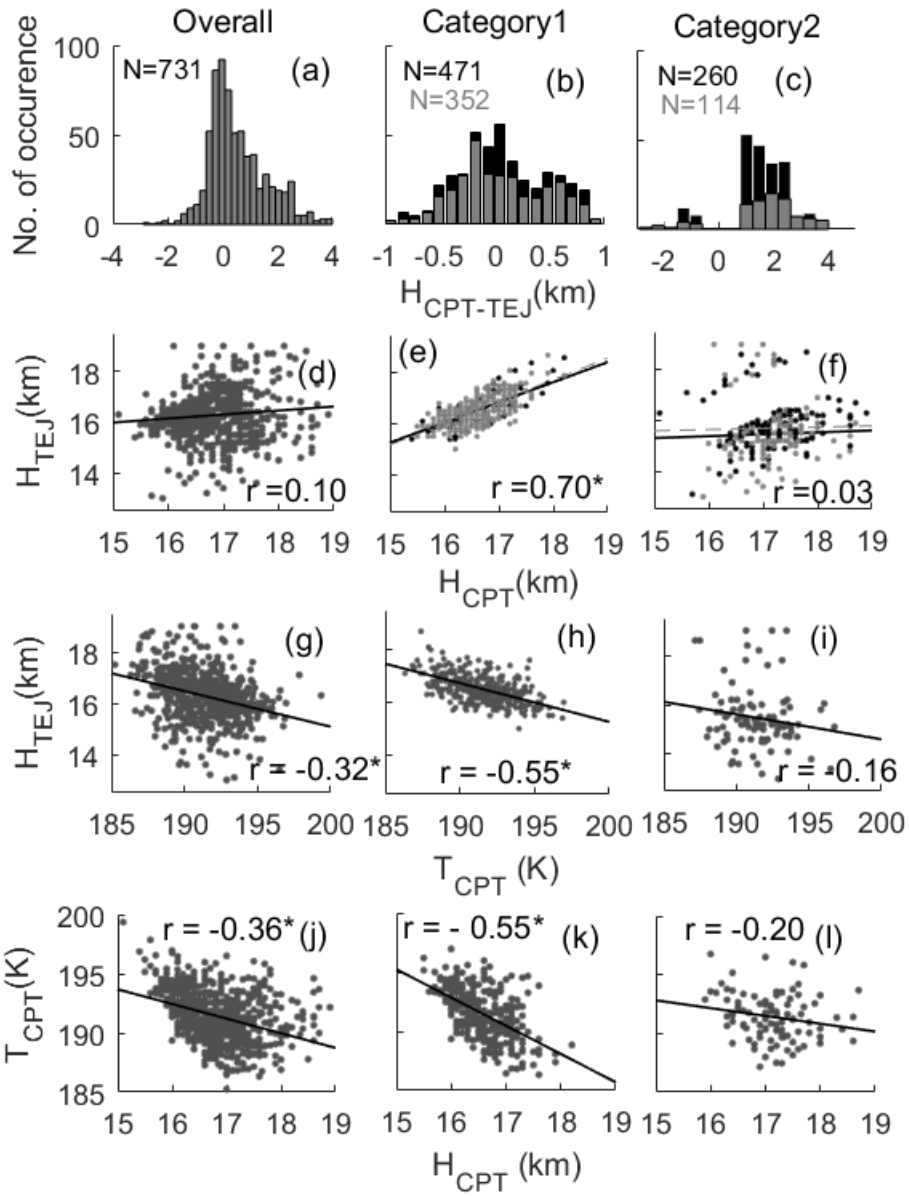

Figure 3. Probability distribution of $H_{CPT-TEJ}$ during (a) overall monsoon, (b) category1, (c) category2. (d-f), (g-i) and (j-l) are the same as (a-c) but for scatter plot between H_{CPT} and H_{TEJ}, H_{TEJ} and T_{CPT}, and H_{CPT} and T_{CPT}, respectively. Grey bars in (b-c) and scatters in (e-f) indicate "close to each other" and "far apart" cases.

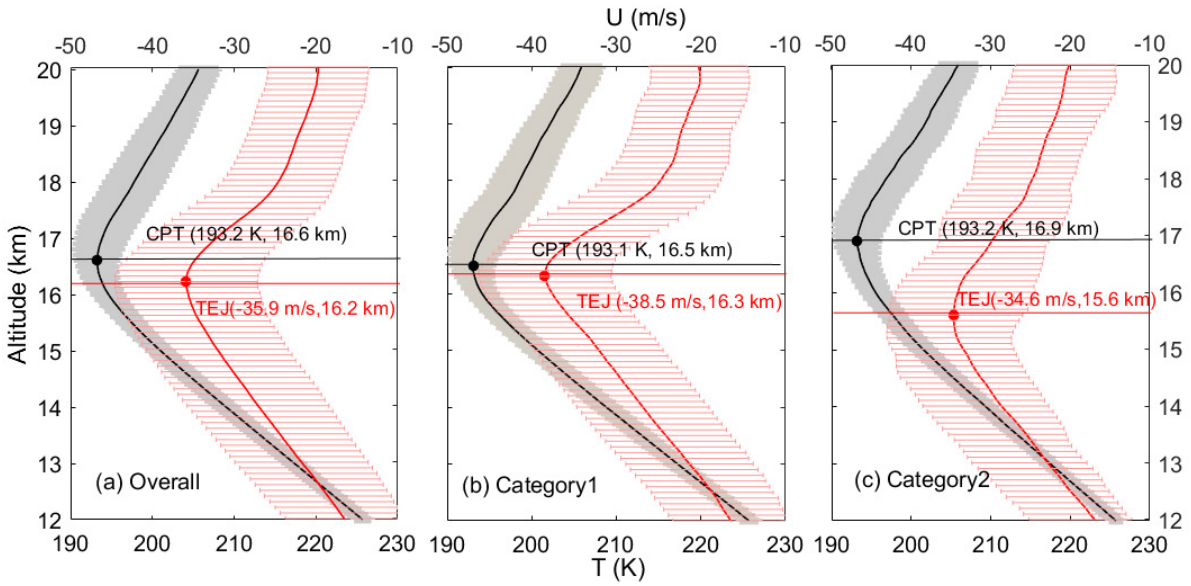

Figure 4. Average profiles of temperature (T; black line) and zonal wind (U; red line) along with their one standard deviation during (a) overall monsoon, (b) category1 and (c) category2. CPT altitude and temperature and TEJ altitude and TEJ peak value are also shown.